RAPID COMMUNICATIONS

PHYSICAL REVIEW C VOLUME 52, NUMBER 4 OCTOBER 1995

Role of the ρ meson in the nonmesonic hypernuclear decay

A. Parreño and A. Ramos
Departament d'Estructura i Constituents de la Matèria, Facultat de Física, Diagonal 647, E-08028 Barcelona, Spain

C. Bennhold
Center of Nuclear Studies, Department of Physics, The George Washington University, Washington, D.C. 20052
(Received 1 June 1995)

The ρ-meson contribution to the $\Lambda N \to NN$ process is studied in the nonmesonic decay of hypernuclei. It is found that the central potential of the ρ exchange is larger than its tensor part and, therefore, must be included. This is in contrast to the π-exchange term which is dominated by the tensor interaction.

PACS number(s): 21.80.+a, 13.75.Ev, 25.80.Pw

It has long been known that the dominant decay mode for all but the lightest hypernuclei is the nonmesonic weak two-body process $\Lambda N \to NN$. In recent years, experimental measurements performed at BNL and KEK have provided new data for previously unmeasured observables, such as the proton asymmetry from the decay of polarized hypernuclei. In terms of hadronic degrees of freedom, the $\Lambda N \to NN$ process initially had been described with a one-pion-exchange potential since the weak $\Lambda N \pi$ vertex is well constrained from the free $\Lambda \to N\pi$ decay. Therefore, this mechanism can straightforwardly model the long-range part of the $\Lambda N \to NN$ interaction. However, models with π exchange alone dramatically fail to reproduce the experimental neutron-to-proton induced ratio Γ_n/Γ_p. Furthermore, the nucleons in the final state emerge with a large momentum of around 400 MeV/c, suggesting that short-range effects may be important.

In order to address this issue, a number of theoretical studies in recent years have investigated the contribution of the ρ meson to the $\Lambda N \to NN$ process [1–3]. Due to the different models employed for the weak $\Lambda N \rho$ vertex these calculations have yielded widely varying results. However, all works until now that have studied the ρ-meson exchange diagram have only included the tensor part of the parity-conserving ρ-exchange term. This was in part motivated by the observation that the central potential of the π-exchange term gives only a negligible contribution. It is the purpose of this paper to demonstrate by explicit calculation that the central part of the ρ exchange is not only nonnegligible but is in fact larger than its tensor interaction. This can be traced to the fact that the ρ-exchange diagram has a much shorter range than the π-exchange potential.

Rather than evaluating the relevant matrix elements in nuclear matter we use a shell model framework in order to include the effects of finite hypernuclear structure as well as possible. For one pion exchange the weak vertex is given by

$$\mathscr{H}_{\Lambda N \pi} = i G_F \mu^2 \bar{\psi}_N (A + B\gamma_5) \boldsymbol{\tau} \boldsymbol{\phi}_\pi \psi_\Lambda , \tag{1}$$

where $G_F \mu^2 = 2.21 \times 10^{-7}$ with μ being the pion mass. The empirical constants $A = 1.05$ and $B = -7.15$, adjusted to the free Λ decay, determine the strength of the parity-violating (PV) and parity-conserving (PC) rates, respectively, and ψ_Λ is a $\tau_3 = -1/2$ field, which is used to enforce the empirical $\Delta I = 1/2$ rule.

For the weak and strong ρ vertices we take [1]

$$\mathscr{H}^W_{\Lambda N \rho} = G_F \mu^2 \bar{\Psi}_N \left(\alpha \gamma^\mu - \beta i \frac{\sigma^{\mu\nu} q_\nu}{2\bar{M}} + \varepsilon \gamma^\mu \gamma_5 \right) \boldsymbol{\tau} \boldsymbol{\rho}_\mu \Psi_\Lambda , \tag{2}$$

$$\mathscr{H}^S_{NN\rho} = \bar{\Psi}_N \left(F_1 \gamma^\mu + i \frac{F_2}{2M} \sigma^{\mu\nu} q_\nu \right) \boldsymbol{\tau} \boldsymbol{\rho}_\mu \Psi_N , \tag{3}$$

respectively, where the four momentum transfer q is directed towards the strong vertex. The strong $NN\rho$ couplings are taken from either the Nijmegen [4] or the Jülich [5] potentials while we employ the methods of Ref. [6] to obtain the weak $\Lambda N \rho$ vertices. For example, the parity-conserving weak vertices are computed by using a pole model that requires the weak meson $\to$ meson and baryon $\to$ baryon transition amplitudes as input. Following the procedure of Ref. [7] the weak vector and axial currents are expressed in terms of $SU(6)_w$ currents. The Hamiltonian is the product of two currents, each belonging to the 35 representation. From the expansion $35 \otimes 35 = 1_s \oplus 35_s \oplus 189_s \oplus 405_s \oplus 35_a \oplus 280_a \oplus \overline{280}_a$ one can associate the symmetric pieces with the parity-conserving Hamiltonian and the antisymmetric pieces with the parity-violating Hamiltonian. Therefore, using $SU(6)_w$ symmetry and enforcing the empirical $\Delta I = 1/2$ rule yields the necessary meson $\to$ meson amplitudes in terms of the $K \to \pi$ amplitude, $\langle M' | H_w | M \rangle \sim \langle \pi | H_w | K \rangle$. Employing partially conserved axial-vector current this amplitude can be related to the physical $K \to \pi\pi$ decay rate via

$$\lim_{q \to 0} \langle \pi\pi | H_{pv} | K \rangle = -\frac{i}{F_\pi} \langle \pi | [F^5_\pi, H_{pv}] | K \rangle = -\frac{i}{2F_\pi} \langle \pi | H_{pc} | K \rangle \tag{4}$$

thus constraining the meson $\to$ meson transition amplitudes. Similarly, the baryon $\to$ baryon amplitudes can be related to the physical free lambda and sigma mesonic decay amplitudes. Details of this method will be presented elsewhere [8]. The strong and weak coupling constants of the ρ used in this paper are given in Table I.

TABLE I. Nijmegen (Jülich) strong and weak coupling constants for the ρ-exchange mechanism. Note that the weak PC coupling constants α and β are calculated with a pole model and thus depend on the values of the strong coupling constants.

Strong	F_1	3.16 (3.25)
	F_2	13.34 (19.82)
Weak	α	−3.80 (−3.91)
	β	−6.77 (−10.56)
	ε	1.09

In order to avoid the complications present in introducing a short-range correlation function in a relativistic matrix element [9] and also for the sake of clarity for the discussion below, we use a nonrelativistic potential for the meson exchanges. Within this framework the ρ-meson contribution is given by

$$M_\rho(\mathbf{q})=\frac{G_F\mu^2}{\mathbf{q}^2+m_\rho^2}\left(F_1\alpha-\frac{(\alpha+\beta)(F_1+F_2)}{4M\bar{M}}(\boldsymbol{\sigma}_1\times\mathbf{q})(\boldsymbol{\sigma}_2\times\mathbf{q})\right.$$
$$\left.+i\frac{\varepsilon(F_1+F_2)}{2M}(\boldsymbol{\sigma}_1\times\boldsymbol{\sigma}_2)\mathbf{q}\right)(\boldsymbol{\tau}_1\boldsymbol{\tau}_2). \tag{5}$$

Using $(\boldsymbol{\sigma}_1\times\mathbf{q})(\boldsymbol{\sigma}_2\times\mathbf{q})=(\boldsymbol{\sigma}_1\boldsymbol{\sigma}_2)\mathbf{q}^2-(\boldsymbol{\sigma}_1\mathbf{q})(\boldsymbol{\sigma}_2\mathbf{q})$ and performing a Fourier transform of $M_\rho(\mathbf{q})$ one obtains the corresponding transition potential in coordinate space, which, as for π exchange, can be divided into central, tensor, and parity-violating pieces

$$V_\rho(\mathbf{r})=V_\rho^C(\mathbf{r})+V_\rho^T(\mathbf{r})+V_\rho^{\mathrm{PV}}(\mathbf{r}). \tag{6}$$

In the case of the ρ meson, the central piece is further decomposed into a spin-independent (SI) and a spin-dependent (SD) part

$$V_\rho^C(\mathbf{r})=V_\rho^{\mathrm{SI}}(\mathbf{r})+V_\rho^{\mathrm{SD}}(\mathbf{r}) \tag{7}$$

with

$$V_\rho^{\mathrm{SI}}(\mathbf{r})=G_F\mu^2F_1\alpha\frac{e^{-m_\rho r}}{4\pi r}(\boldsymbol{\tau}_1\boldsymbol{\tau}_2), \tag{8}$$

$$V_\rho^{\mathrm{SD}}(\mathbf{r})=G_F\mu^2\frac{(\alpha+\beta)(F_1+F_2)}{4M\bar{M}}\frac{2}{3}\left(m_\rho^2\frac{e^{-m_\rho r}}{4\pi r}-\delta(\mathbf{r})\right)$$
$$\times(\boldsymbol{\sigma}_1\boldsymbol{\sigma}_2)(\boldsymbol{\tau}_1\boldsymbol{\tau}_2). \tag{9}$$

The tensor and parity-violating pieces of the transition potential are given by

$$V_\rho^T(\mathbf{r})=-G_F\mu^2\frac{(\alpha+\beta)(F_1+F_2)}{4M\bar{M}}\frac{1}{3}T(m_\rho r)\left(m_\rho^2\frac{e^{-m_\rho r}}{4\pi r}\right)$$
$$\times S_{12}(\hat{r})(\boldsymbol{\tau}_1\boldsymbol{\tau}_2), \tag{10}$$

$$V_\rho^{\mathrm{PV}}(\mathbf{r})=-G_F\mu^2\frac{\varepsilon(F_1+F_2)}{2M}m_\rho V(m_\rho r)\frac{e^{-m_\rho r}}{4\pi r}$$
$$\times\hat{\mathbf{r}}(\boldsymbol{\sigma}_1\times\boldsymbol{\sigma}_2)(\boldsymbol{\tau}_1\boldsymbol{\tau}_2), \tag{11}$$

respectively, where the following definitions

$$T(m_\rho r)=\left(1+\frac{3}{m_\rho r}+\frac{3}{(m_\rho r)^2}\right),$$

$$S_{12}(\hat{\mathbf{r}})=3(\boldsymbol{\sigma}_1\hat{\mathbf{r}})(\boldsymbol{\sigma}_2\hat{\mathbf{r}})-\boldsymbol{\sigma}_1\boldsymbol{\sigma}_2,$$

$$V(m_\rho r)=1+\frac{1}{m_\rho r}$$

have been used. We note that, since the PC constants α, β for the ρ meson have the same sign as the constant B for the pion, the ρ tensor potential interferes destructively with that of the pion, as in the case of the strong NN interaction.

A monopole form factor $F(\mathbf{q}^2)=(\Lambda_c^2-m^2)/(\Lambda_c^2+\mathbf{q}^2)$, with m being the meson mass, is used at each vertex, where the value of the cutoff Λ_c depends on the meson. We take the values of the Jülich YN interaction [5] ($\Lambda_\pi=1.3$ GeV, $\Lambda_\rho=1.4$ GeV), since the Nijmegen model distinguishes form factors only in terms of the transition channel. To account for the ΛN correlations, which are absent in the independent particle model, one has to include a correlation function, for which we take the parametrization

$$f(r)=(1-e^{-r^2/a^2})^n+br^2e^{-r^2/c^2}, \tag{12}$$

where $r=|\mathbf{x}-\mathbf{y}|$. The values $a=0.5$, $b=0.25$, $c=1.28$, and $n=2$ provide an average spin-independent correlation function that represents a good approximation to the results obtained in microscopic G-matrix calculations in finite hypernuclei [10] using the Nijmegen YN interactions [4]. Final state interactions are taken into account via an average NN correlation function in the final state, for which we take $f_{\mathrm{FSI}}(r)=1-j_0(q_c r)$, with $q_c=3.93\ \mathrm{fm}^{-1}$ [11]. We note that, in principle, both initial and final state correlations are state dependent and, therefore, different correlation functions should be used for the various transitions, as was done in Ref. [2]. However, for the more qualitative results presented here we neglect these differences that should be included in future studies.

The results of our calculations are shown in Tables II–IV where the nonmesonic decay rate of ${}^{12}_{\Lambda}\mathrm{C}$ is given in units of the free lambda decay rate. Table II presents our results for π exchange alone, demonstrating the effects of short-range correlations (SRC), form factors (FF), and final-state interactions (FSI) separately for the central, tensor, and parity-violating potentials. The free central term is reduced dramatically by SRC, however, most of the free central potential is in fact due to the δ function which is completely eliminated by SRC. Ignoring the δ function, the central part is reduced by a factor of 2, from 0.006 to 0.003. Including SRC, FF, and

TABLE II. π-exchange contribution to the $\Lambda N \rightarrow NN$ decay rate of ${}^{12}_{\Lambda}$C. The values in brackets are obtained when the δ function in the central channel is ignored.

	Free	SRC	SRC, FF	SRC, FF, FSI
C	0.288 (0.006)	0.003	0.013	0.004
T	0.818	0.739	0.598	0.645
PV	0.470	0.379	0.327	0.354
Γ	1.576 (1.294)	1.121	0.938	1.003

FSI reduces the total central potential by a factor of 70, from 0.288 to 0.004. In contrast, the tensor interaction of the π-exchange diagram is only reduced by 10% by SRC and by 20% once FF and FSI are applied as well. Therefore, the contribution of the central term amounts to less than 0.5% of the total π-exchange rate. This behavior has been found and discussed by other authors as well [1,2,6]. We note, however, that our PV potential yields about 30% of the π-exchange rate, at variance with older nuclear matter results that reported negligible PV rates [1].

Our results for the ρ-meson exchange contribution are shown in Table III. As noted before, the central potential can now be divided into a spin-dependent (SD) and spin-independent (SI) piece, which are shown separately. In contrast to the pion case, the factor m_ρ^2 in front of the Yukawa function in the SD central part of Eq. (9) enhances this contribution which then becomes comparable in magnitude to the piece containing the delta function. The two terms interfere destructively, as can be seen from the large value of 3.155 (without SRC, FF, or FSI), obtained when the δ function is removed. Even with this interference, the SD central part is larger than the tensor contribution. To understand the origin for the different ratio of central to tensor transition strengths in the π- and ρ-exchange mechanisms we show in Fig. 1 the integrands of the SD central (without the δ function) and tensor amplitudes at a fixed relative outgoing momentum. The tensor amplitude induces $S \rightarrow D$ transitions and, therefore, is governed by the Bessel function $j_2(k_r r)$, describing the NN motion in the final state. Since j_2 vanishes at the origin it eliminates strength from the tensor potential at short distances. Due to its shorter range, the tensor contribution of the ρ is reduced more than in the case of the pion. The central piece, on the other hand, is governed by $j_0(k_r r)$ and, thus, the potential at short distances is not suppressed. However, due to the smaller value of m_π, the function $j_0(k_r r)$ oscillates once in the effective range of the pion

TABLE III. ρ-exchange contribution to the $\Lambda N \rightarrow NN$ decay rate of ${}^{12}_{\Lambda}$C using the Nijmegen constants. The values in brackets are obtained when the δ function of the central channel is ignored.

	Free	SRC	SRC, FF	SRC, FF, FSI
C (SI)	0.774	0.088	0.051	0.033
C (SD)	0.234 (3.155)	0.361	0.015	0.023
C (Total)	0.669 (5.247)	0.599	0.090	0.079
T	0.156	0.065	0.022	0.023
PV	1.7×10^{-3}	4.7×10^{-4}	1.8×10^{-4}	1.7×10^{-4}
Γ	0.828 (5.406)	0.665	0.112	0.103

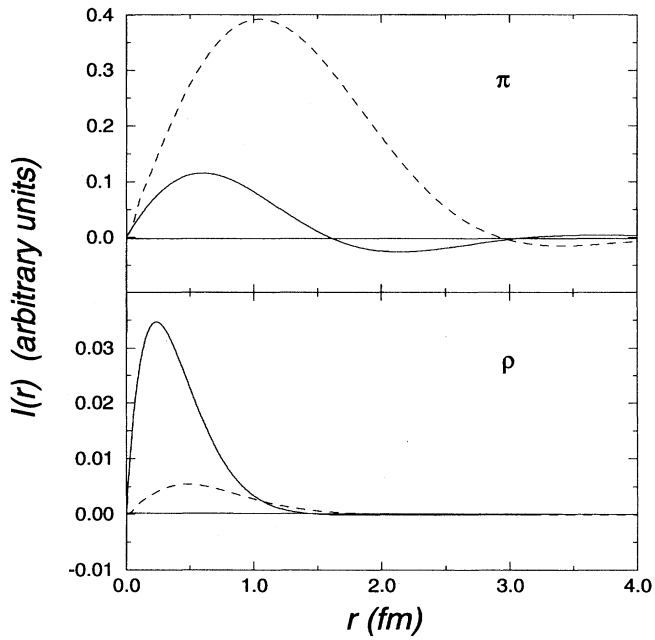

FIG. 1. Integrand of the free transition amplitude, in arbitrary units, at fixed outgoing relative momentum ($k_r = 390$ MeV/c) for the spin-dependent central potential without the δ function (solid line) and for the tensor potential (dashed line). Upper part: pion exchange. Lower part: rho exchange.

central potential, leading to a reduction of its central contribution relative to the tensor one.

Returning to our discussion of the ρ contribution, the results shown in Table III illustrate that SRC reduce both the central SI and the SD part without δ function by almost a factor of 10, compared to a factor of 2 in the π case, again reflecting the much shorter range of the ρ-exchange diagram. Similarly, the tensor interaction of the ρ is reduced by a factor of 2.5, compared to a 10% reduction in the π case, as soon as SRC are included. The additional inclusion of FF and FSI further reduces both the central and tensor rates by substantial amounts. The final result of the central contribution exceeds the tensor term by more than a factor of 3. We emphasize the relative contribution of the central and the tensor parts of the ρ exchange; clearly, all of these potentials scale with the magnitude of the weak PC $\Lambda N \rho$-coupling constant which is model dependent. Due to the particular model we employ, the PV part of the ρ exchange is negligible.

One may think that, due to the much shorter range of the ρ potential, it would be very sensitive to the details of the short-range correlation function. This is indeed the case, since we obtain a value for the total ρ rate of 0.673 (0.373) when we use a realistic correlation function obtained from a G-matrix calculation [9] with the Nijmegen soft-core (hard-core) interaction. However, as soon as form factors and final state interactions, which provide further suppression at short distances, are included, the ρ rate reduces to 0.114 and 0.101, for the Nijmegen soft and hard core, respectively, very similar to the value 0.103 obtained with our spin-independent parametrization of Eq. (12).

To further illustrate the effect of the different model ingredients on the π and ρ rates, we present in Fig. 2 the

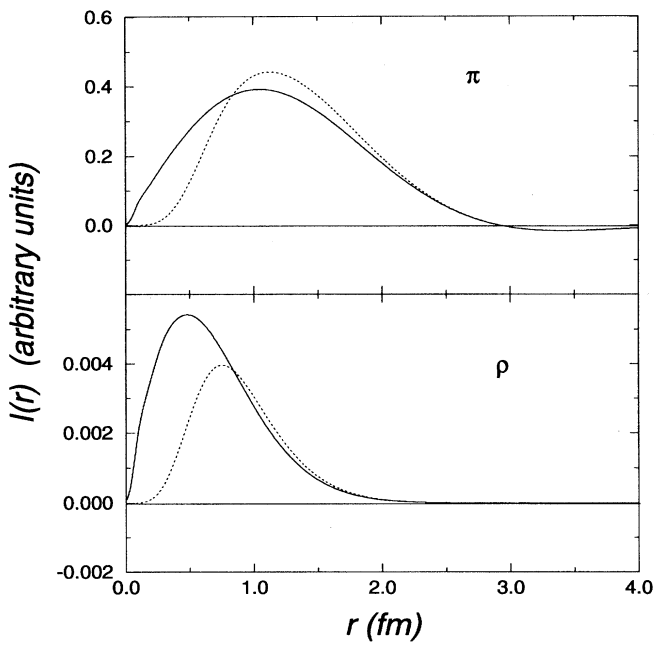

FIG. 2. Illustration of the effects of SRC, FF, and FSI in the tensor transition amplitude. The solid line shows the free tensor integrand as in Fig. 1 and the dotted line includes the effects of SRC, FF, and FSI. Upper part: pion exchange. Lower part: rho exchange.

integrands of their tensor amplitudes at a fixed relative outgoing momentum. The solid line corresponds to the free case, in which SRC, FF, and FSI effects are ignored. Clearly, the integrand of the ρ exchange peaks sooner ($\approx$ 0.5 fm) and drops off faster, reaching zero at around 2 fm, than the integrand for the π exchange which peaks around 1 fm and drops to zero around 3 fm. It therefore comes as no surprise that including SRC leads to much stronger reduction for the ρ than for the π contribution. The dotted line shown in Fig. 2 further confirms this finding by demonstrating the effects of SRC, FF and FSI on the free integrand.

Finally, Table IV presents our results for the π and ρ exchanges combined. Since both the $\Lambda N\pi$ and the $\Lambda N\rho$ couplings are obtained within the same model there is no sign ambiguity. We find a destructive interference between the two mesons, leading to a 17% reduction compared to the rate calculated with π exchange only. Ignoring the central pieces of the ρ exchange mechanism would give a reduction of 22%. Clearly, this 5% difference is a reflection of the particular model employed for the weak $\Lambda N\rho$ vertex. In fact, this effect is already slightly more pronounced when we use the Jülich model for the strong coupling constants which, in turn, produce different predictions for the weak constants, as shown in Table I. The result for the $\pi+\rho$ decay rate with the Jülich constants, shown in brackets in Table IV, is 0.770, which is 23% smaller than for π exchange only. The reduction would amount to 35% if the central contributions were ignored. Furthermore, the findings reported here for the ρ-meson contribution hold for the other vector mesons, such as the K^* and the ω, as well, which can have larger couplings [8].

TABLE IV. π and ρ exchange contribution to the $\Lambda N \rightarrow NN$ decay rate of ${}^{12}_{\Lambda}$C.

	π	ρ	$\pi+\rho$
		Nijmegen (Jülich)	Nijmegen (Jülich)
C (SI)		0.033 (0.037)	0.033 (0.037)
C (SD)	0.004	0.023 (0.086)	0.008 (0.053)
C (Total)	0.004	0.079 (0.169)	0.054 (0.125)
T	0.645	0.023 (0.086)	0.423 (0.273)
PV	0.354	1.7×10^{-4} (3.3×10^{-4})	0.360 (0.373)
Γ	1.003	0.103 (0.256)	0.836 (0.770)

The neutron to proton induced ratio Γ_n/Γ_p, on the other hand, is increased by about 20%, from a value of 0.13 for π exchange only to 0.16 when the ρ is included. Using the Jülich constants the $\pi+\rho$ value becomes 0.19, which represents an increase of almost 40%. While this is nowhere near an increase that would be needed to explain experimental data [12], it is clearly a reflection of the fact that the tensor interaction of the ρ exchange is not as dominant as it is in the π case.

Our results for the rates calculated with the ρ meson are quite different from previous studies [1–3]. This is not only due to the omission of the central potential in the ρ-exchange diagram, but even more so can be traced to the different models used for the weak $\Lambda N\rho$ coupling constants. In contrast to our approach, Refs. [1,2] employed a factorization model which gave large couplings and did not fix the relative sign between π and ρ exchange. References [1,3] also employed a pole model which is similar in spirit to the one used here. However, among other differences from previous studies, the strong couplings needed as input in our pole model were taken from realistic YN potentials. What has been neglected in all calculations until now is the possibility of the weak $\Lambda N\rho$ vertex having significant $\Delta I=3/2$ contributions, as has been suggested recently in Ref. [15]. Clearly, further work is required to understand which model is appropriate to describe the weak $\Delta S=1$ baryon-meson couplings.

In conclusion, we have demonstrated that the central potential of the ρ-meson contribution to the $\Lambda N \rightarrow NN$ process cannot be neglected and is in fact larger than its tensor part. Due to the very different ranges of the π and the ρ exchange their contributions are modified differently when short-range correlations and form factors are included. In view of a number of more recent theoretical efforts that increase the complexity of the $\Lambda N \rightarrow NN$ reaction mechanism by calculating correlated 2π exchanges, through the coupling to the isoscalar σ meson [13] or via strange $\Lambda N \rightarrow \Sigma N$ mixing [14], it is imperative that all parts of the ρ-meson potential be included first.

This work has been partially supported by DGICYT Contract No. PB92-0761 (Spain) and by U.S.-DOE Grant No. DE-FG02-95-ER40907. A. Ramos gratefully acknowledges support during her stay at the George Washington University where part of this work was completed. A. Parreño acknowledges support from the Spanish Ministerio de Educación y Ciencia.

[1] B.H.J. McKellar and B.F. Gibson, Phys. Rev. C **30**, 322 (1984).
[2] K. Takeuchi, H. Takaki, and H. Bandō, Prog. Theor. Phys. **73**, 841 (1985).
[3] G. Nardulli, Phys. Rev. C **38**, 832 (1988).
[4] M.M. Nagels, T.A. Rijken, and J.J. de Swart, Phys. Rev. D **15**, 2547 (1977); P.M.M. Maessen, T.A. Rijken, and J.J. de Swart, Phys. Rev. C **40**, 2226 (1989).
[5] B. Holzenkamp, K. Holinde, and J. Speth, Nucl. Phys. **A500**, 485 (1989).
[6] J.F. Dubach, Nucl. Phys. **A450**, 71c (1986); L. de la Torre, Ph.D. thesis, Univ. of Massachusetts, 1982; J.F. Dubach *et al.*, University of Massachusetts Report No. UMHEP-366 (1992).
[7] A.P. Balanchandran *et al.*, Phys. Rev. **153**, 1553 (1967).
[8] A. Parreño, A. Ramos, and C. Bennhold (unpublished).
[9] A. Parreño, A. Ramos, C. Bennhold, and D. Halderson, in *Dynamical Features of Nuclei and Finite Fermi Systems*, edited by X. Viñas, M. Pi, and A. Ramos (World Scientific, Singapore, 1994), p. 318; A. Parreño, A. Ramos, and E. Oset, Phys. Rev. C **51**, 2477 (1995).
[10] D. Halderson, Phys. Rev. C **48**, 581 (1993).
[11] W. Weise, Nucl. Phys. **A278**, 402 (1977).
[12] J.J. Szymanski *et al.*, Phys. Rev. C **43**, 849 (1991).
[13] K. Itonaga, T. Ueda, and T. Motoba, Nucl. Phys. **A585**, 165c (1995).
[14] M. Shmatikov, Nucl. Phys. **A580**, 538 (1994).
[15] K. Maltman and M. Shmatikov, Phys. Rev. C **51**, 1576 (1995).